Journal of Alloys and Compounds 508 (2010) 384–390

Contents lists available at ScienceDirect

Journal of Alloys and Compounds

journal homepage: www.elsevier.com/locate/jallcom

Bioactivity and corrosion properties of novel coatings containing strontium by micro-arc oxidation

Kuan-Chen Kung[a], Tzer-Min Lee[b,*], Truan-Sheng Lui[a]

[a] Department of Materials Science and Engineering, National Cheng Kung University, Tainan, Taiwan
[b] Institute of Oral Medicine, National Cheng Kung University, Tainan, Taiwan

ARTICLE INFO

Article history:
Received 8 July 2010
Accepted 14 August 2010
Available online 24 August 2010

Keywords:
Bioactivity
Corrosion
Micro-arc oxidation (MAO)
Strontium
Coatings

ABSTRACT

Pure titanium (Ti) and titanium alloys are considered as bio-inert materials in clinical use. Bioactivity is the ability to induce bone-like apatite on the material surface. The micro-arc oxidation (MAO) technique is an effective method for improving the surface properties of titanium. The aim of this study was to investigate the bioactivity and corrosion behavior of MAO coatings containing strontium, which is beneficial for biological performance. The bioactivity of materials was evaluated based on the ability to induce a bond-like apatite layer on the surface in simulated body fluid (SBF), as proposed by Kokubo et al. After the materials were soaked in SBF for 1 day, precipitates formed on the surface of MAO coating. The surface of MAO coatings was completely covered with precipitates after 7 days. The precipitates, which were found to be composed of fiber structures, were identified as the apatite phase using thin film X-ray diffraction (TF-XRD). The results show that MAO coatings containing strontium can induce the formation of an apatite layer on their surface. In the potentiodynamic test, MAO coatings exhibited a more noble corrosion potential (E_{corr}) than that of titanium in SBF. In the passive region, the current density of MAO coatings was lower than that of titanium. All findings in this study indicated that MAO coatings containing strontium have good bioactivity and corrosion resistance for clinical applications.

© 2010 Elsevier B.V. All rights reserved.

1. Introduction

Implants made of titanium and its alloys are widely used in dental and orthopedic fields due to their excellent properties, including high strength-to-weight ratio, low toxicity, and favorable mechanical properties compared to other metals such as stainless steel [1]. The corrosion resistance of titanium has been attributed to the existence of a thin and stable passivating oxide layer of TiO_2 [2]. However, due to the bio-inert properties of a natural oxide layer, it is difficult to achieve a chemical bond with bone tissue and to form a new bond on the surface [3]. To improve biocompatibility, surface treatments are often used to modify the chemical and morphological properties of metal. For example, the sandblasted and acid-etched (SLA) surface of implants has better bonding strength to bone than that of the machined surface of titanium implants *in vivo* [4]. In recent years, the micro-arc oxidation (MAO, also named anodic spark oxidation or plasma electrolytic oxidation) process has attracted considerable attention because it combines the chemical and morphological modification of titanium surfaces in a single process step. The MAO technique can be used to easily control surface properties, such as oxide thickness, chemical composition, pore size, and roughness. The MAO method produces uniformly porous oxide coatings on implant surfaces with complex geometries, such as dental root implants with screws.

After an artificial material is soaked in simulated body fluid (SBF) or implanted in a body environment, the formation of bone-like apatite layer on its surface indicates that it is biocompatible and bond to bone. Previous studies indicated that the formation of bone-like apatite on the surface of materials in SBF allows the direct-to-bone contact *in vivo* [5–7]. Therefore, the bioactivity of implant materials can be evaluated based on the ability to induce a bone-like apatite layer on the surface in SBF.

Recently, strontium-substituted calcium phosphates have been developed [8,9]. Strontium (Sr), a divalent cation, is used in clinical applications for osteoporotic patients. The clinical success of strontium salts, such as strontium ranelate, was attributed to the prevention of bone loss via the depression of bone resorption and the maintenance of bone formation. Strontium-containing hydroxyapatite (Sr-HA) was designed as a filling material to improve the biocompatibility of bone cement [10]. Capuccini et al. employed pulsed-laser deposition to prepare Sr-HA coatings on titanium substrates [11]. *In vitro*, the presence of strontium in the coating enhances osteoblast activity and differentiation, whereas it inhibits osteoclast production and proliferation.

* Corresponding author. Tel.: +886 6 2353535x5361; fax: +886 6 2359885.
E-mail address: tmlee@mail.ncku.edu.tw (T.-M. Lee).

0925-8388/$ – see front matter © 2010 Elsevier B.V. All rights reserved.
doi:10.1016/j.jallcom.2010.08.057

Table 1
Composition of the MAO electrolyte.

Specimen	Solution composition (M)		
	$NaH_2PO_4{\cdot}H_2O$	$Ca(CH_3COO)_2{\cdot}H_2O$	$Sr(OH)_2{\cdot}8H_2O$
CP	0.06	0.13	0
CPS1	0.06	0.1287	0.0013
CPS5	0.06	0.1235	0.0065
CPS10	0.06	0.117	0.013

In the present study, MAO was used to modify a titanium surface in aqueous electrolytes, allowing strontium, calcium, and phosphorus to be incorporated into a titanium oxide matrix in a single anodic oxidation. The MAO coatings were exposed to simulated body fluid, and changes in their characteristics, especially the formation of apatite film, were analyzed. The electrochemical properties of the MAO coatings were analyzed and compared to those of titanium using the potentiodynamic polarization test.

2. Materials and methods

2.1. Preparation of specimens

Disks of medical grade titanium (commercially pure Ti, Grade 2, ASTM F-67), measuring 12.7 mm in diameter and 2 mm in thickness, were selected as substrate. The substrates were ground using silicon carbide papers, then ultrasonically cleaned in acetone, ethanol, and de-ionized water prior to micro-arc oxidation. Four kinds of electrolyte were applied to modify the composition of MAO coatings. The compositions of the electrolytes are shown in Table 1. The MAO electrolyte was prepared by dissolving sodium phosphate monobasic monohydrate ($NaH_2PO_4{\cdot}H_2O$), calcium acetate hydrate ($Ca(CH_3COO)_2{\cdot}H_2O$), and strontium hydroxide 8-hydrate ($Sr(OH)_2{\cdot}8H_2O$) in de-ionized water. The specimens were anodized with a DC power supply (GPS-60H15S, GW) for MAO treatment. The specimen was used as the anode, and a stainless steel plate was used as the cathode in the electrochemical cell. The samples were treated with an applied voltage of 350 V for 1 min, and the electrolyte temperature was maintained at 25 °C by a circulating water system. After MAO treatment, the samples were sequentially rinsed with acetone, ethanol, and de-ionized water, and then dried in oven. In Table 1, the MAO specimens are denoted as CP, CPS1, CPS5, and CPS10 according to the strontium content in the electrolyte. The elemental composition and thickness of MAO coatings are shown in Table 2.

2.2. Characterization of MAO coatings after being soaked in simulated body fluid

The MAO coatings were soaked in simulated body fluid (SBF) with a surface area to solution volume ratio of 0.1 cm^{-1} [5]. The ion concentrations were almost equal to human plasma, as shown in Table 3. The SBF was kept at pH 7.4 and maintained at 37 °C. The characteristics of MAO coatings were evaluated after 1, 3, and 7 days of immersion. The MAO coatings were identified using thin film X-ray diffraction (TF-XRD, Rigaku D/Max) with a scan speed of 4° min^{-1} in the 2θ angle of 20° and 80°. The surface morphology of the specimens was observed using a scanning electron microscope (SEM, JEOL JSM-6390LV) with an energy dispersive X-ray spectrometer (EDX, Oxford INCA/350) for chemical analysis. The calcium, phosphorus, and strontium concentrations of solutions were determined using inductively coupled plasma optical emission spectroscopy (ICP-OES, JY-Ultima 2000).

2.3. Corrosion test

The potentiodynamic polarization test was conducted in SBF (pH 7.4) at 37 °C. The specimens were used as the working electrode in the electrolyte. An Ag/AgCl electrode was used as the reference electrode, and a platinum plate served as the counter electrode. A potentiostat (Autolab PGAST 30), linked to a computer for data acquisition, was used for the experiments. Prior to and during testing, the non-stirred medium was purged with pure nitrogen gas in the electrochemical cell. The specimens were placed into the SBF and equilibrated in the test solution for 1 h prior to generation polarization. The open circuit potential (OCP) was also recorded as a function of immersion period. In the potentiodynamic polarization test, the beginning potential was set at 700 mV active to the rest potential and the scan rate was 5 mV min^{-1} in the noble direction. The scan was stopped when the applied voltage reached 5.0 V (Ag/AgCl). The polarization curves were measured at least in triplicate, with independent samples and fresh solution used in each test.

3. Results

3.1. Morphology of MAO coating surface

Fig. 1(a)–(d) shows the microstructures of the MAO coatings morphology obtained from SEM observation. The open pores were characteristically produced by the spark discharge in the MAO process. The four kinds of specimens show uniform surface morphologies. The insets were recorded for a 30° tilt angle. The coatings have a three-dimensional structure.

3.2. Characteristics of MAO coatings after immersion in simulated body fluid

Few precipitates formed on the surfaces of MAO coatings after immersion for 1 day. A porous structure was observed for the four kinds of MAO coatings. The surface morphologies of MAO coatings after 7 days of immersion are shown in Fig. 2. The surfaces of the four kinds of MAO coating were almost completely covered with precipitates. The surface of titanium was not covered with precipitates after immersion for 7 days. The precipitates were found to be composed of fiber structures, as shown in the insets. As shown in Fig. 3, the CPS1 specimens were identified using TF-XRD after being soaked in SBF for various periods of time. The peaks were identified as apatite; the peak intensities increased with increasing immersion time. The broad peaks are attributed to a defective structure. The TF-XRD patterns of the four kinds of MAO coating specimen after immersion in SBF for 7 days are shown in Fig. 4. The XRD patterns of MAO coatings with various levels of strontium had similar trends.

Fig. 5 shows the ion concentration, determined from ICP-OES, of the test immersion solution of MAO coatings. The ion concentration of calcium and phosphorous decreased with immersion time. As shown in Fig. 5(c), the increase in Sr concentration as a function of time was observed for all four kinds of MAO coatings containing strontium throughout the 0–7 day immersion period. This indicates

Table 2
Elemental compositions and thickness of MAO coatings.

Specimen	EDX results (wt%)					Thickness (μm)
	Ti	O	Ca	P	Sr	
CP	45.02	48.36	3.69	2.93	0	3.72
CPS1	45.18	48.13	3.67	2.87	0.15	3.70
CPS5	45.21	48.03	3.40	2.81	0.55	3.79
CPS10	45.47	47.85	3.19	2.55	0.94	3.74

Table 3
Ion concentration (mM) of simulated body fluid (SBF).

	Na^+	K^+	Ca^{2+}	Mg^{2+}	Cl^-	HCO_3^-	HPO_4^{2-}
SBF	142.0	5.0	2.5	1.5	148.8	4.2	1.0
Blood	142.0	5.0	2.5	1.5	103.0	27.0	1.0

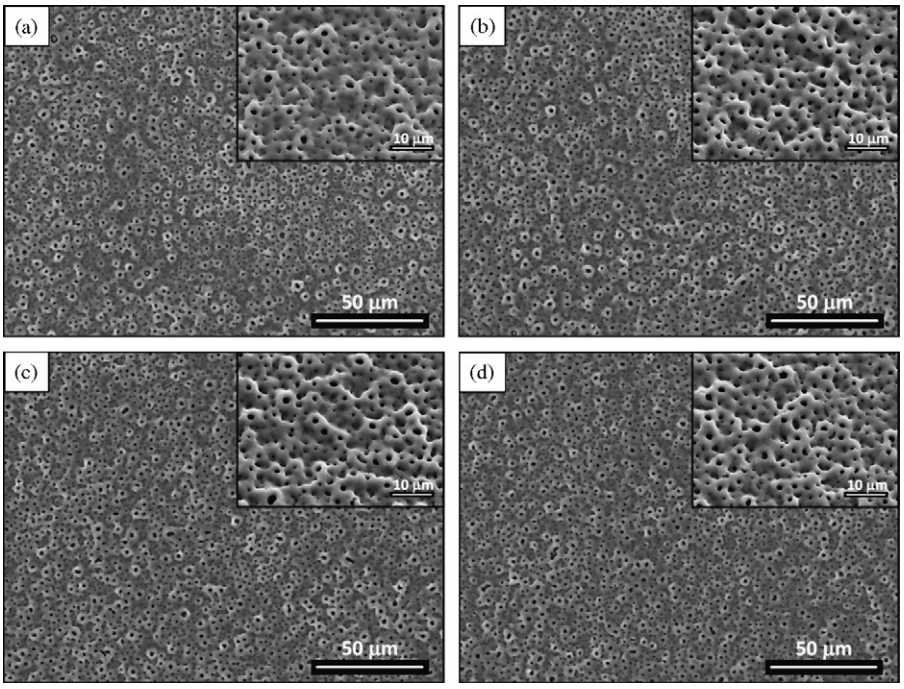

Fig. 1. Morphologies of the MAO coatings. (a) CP, (b) CPS1, (c) CPS5, and (d) CPS10. Insets were recorded at a tilt of 30°.

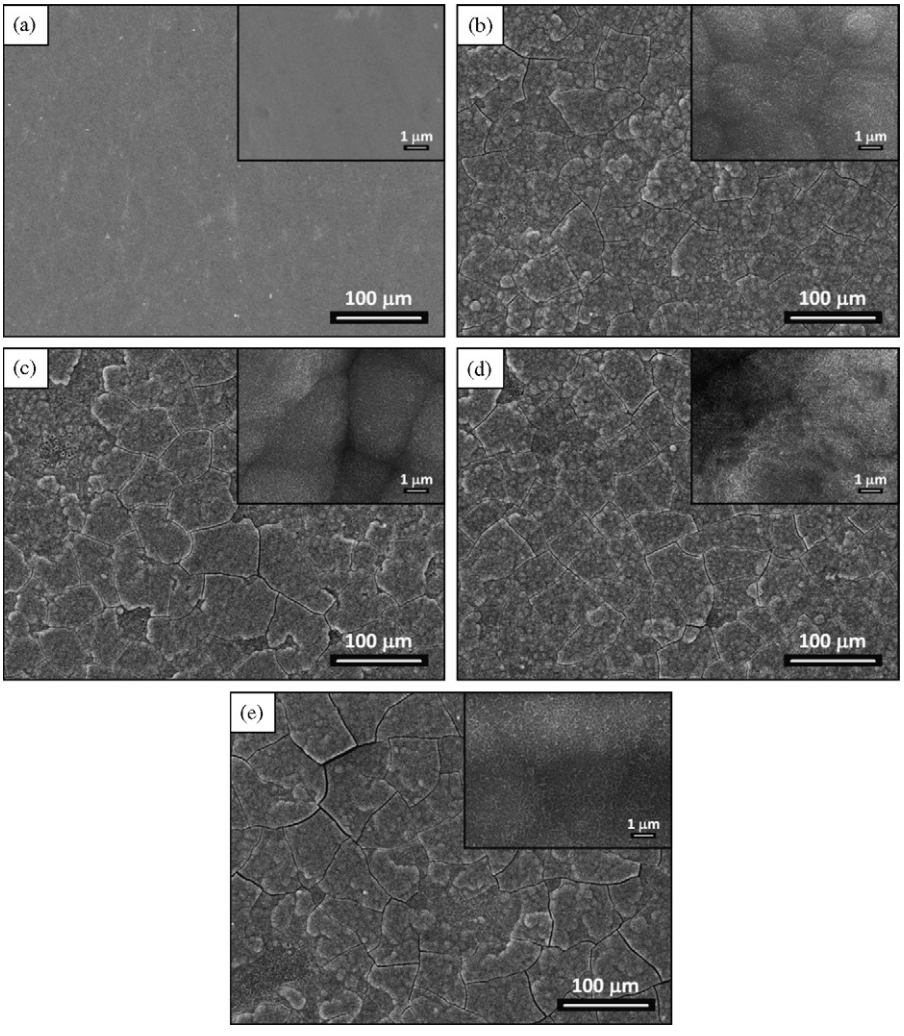

Fig. 2. SEM images of MAO coatings soaked in SBF for 7 days. (a) Ti, (b) CP, (c) CPS1, (d) CPS5, and (e) CPS10.

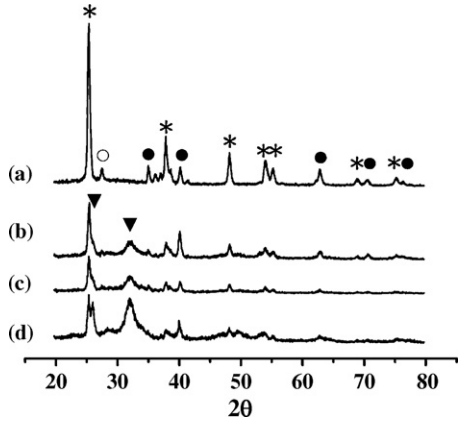

Fig. 3. TF-XRD patterns of CPS1 soaked in SBF for 1, 3, and 7 days. (a) 0 day, (b) 1 day, (c) 3 days, and (d) 7 days. (*) Anatase; (○) rutile; (●) titanium; (▼) apatite.

that strontium was released from MAO coatings, and that calcium and phosphorus ions precipitated on the coatings surface. The precipitate was identified as the apatite phase using TF-XRD. As shown in Fig. 6, the surface compositions of MAO coatings were measured by EDX analysis. The content of calcium and phosphorus significantly increased from day 0 to day 1. However, the content of strontium decreased from day 0 to day 3 and became steady thereafter. These results are consistent with the formation of an apatite layer on the surface of MAO coating exposed to SBF. The precipitate of the apatite layer, mainly composed of calcium and phosphorus, increased the signal of calcium and phosphorus but decreased the signal of strontium.

3.3. Corrosion behavior of MAO coatings

The potential versus time curves from the OCP test can be used to obtain the rest potential. The test solution of SBF was carried out at 37 °C and pH 7.4. The OCP curves of specimens are shown in Fig. 7. It is clear that the OCP values of MAO coatings decreased with increasing time. However, the OCP values of titanium specimens increased with increasing time. This suggests that MAO coatings are not stable in SBF. Although a precipitate of the apatite layer was measured by SEM and TF-XRD, calcium, phosphorus and strontium were released from MAO coatings when the specimens were exposed to SBF. The decrease of OCP for MAO coatings in the initial stage indicates that the MAO coatings are not stable in the initial stage. The potentiodynamic polarization curve of specimens

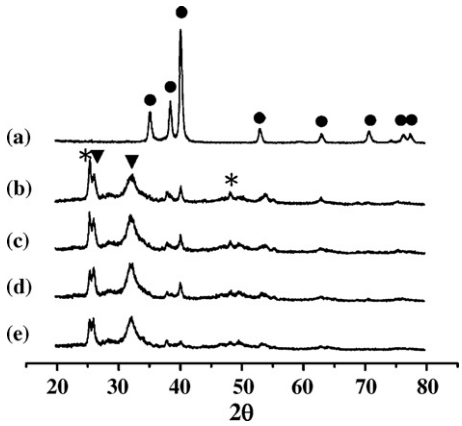

Fig. 4. TF-XRD patterns of MAO coatings containing various levels of strontium soaked in SBF for 7 days. (a) Ti, (b) CP, (c) CPS1, (d) CPS5, and (e) CPS10. (*) Anatase; (●) titanium; (▼) apatite.

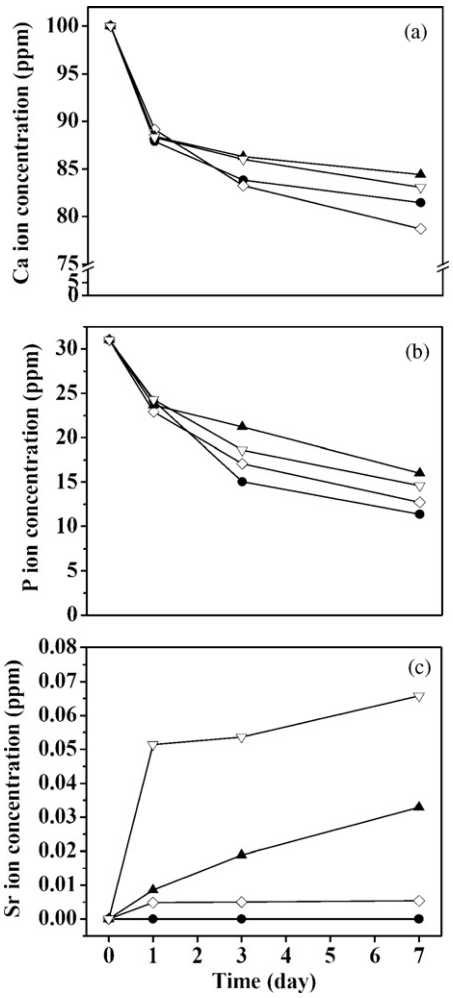

Fig. 5. Ion concentrations of calcium, phosphorus, and strontium in SBF as a function of immersion time of MAO coatings. (a) Calcium, (b) phosphorous, and (c) strontium. (●) CP; (◊) CPS1; (▲) CPS5; (▽) CPS10.

is shown in Fig. 8. The polarization curves of MAO coatings are similar. As shown in Fig. 8, the polarization curves show a passive region. Compared to titanium, the MAO coatings exhibited lower current density in the passive region. The corrosion potentials obtained from the potentiodynamic polarization curves are shown in Fig. 9. The corrosion potential (E_{corr}) of MAO coatings was more noble than that of as-received titanium. The corrosion properties of MAO coatings containing various levels of strontium were similar to those of the CP specimen.

4. Discussion

There are many modification techniques for improving the biocompatibility of titanium. They change the structure, chemical composition, and morphology by depositing a coating on the surface of titanium. The MAO technique combines the chemical and morphological modification of titanium implant surfaces in a single process. MAO produces porous and uniform oxide coatings on implant surfaces with complex geometries, such as dental root implants. Various electrolytic solutions are used to anodize titanium, and the coating composition is mainly determined by the electrolyte constituents. Nan et al. prepared strontium-doped hydroxyapatite film using an electrochemical oxidation method [12]. In the present study, the strontium, calcium, and phosphorus in the electrolytes were incorporated into the coatings during

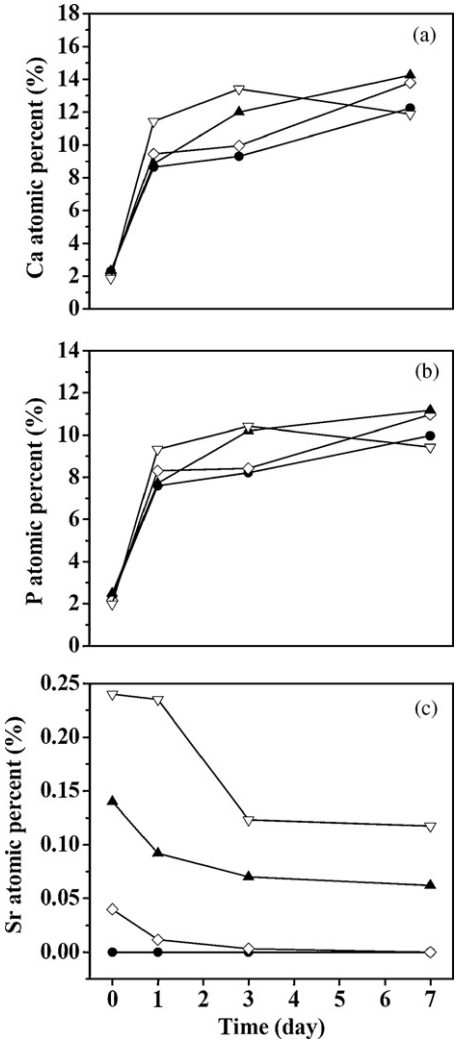

Fig. 6. Elemental composition of calcium, phosphorus, and strontium of MAO coating surfaces measured by EDX for various soaking periods. (a) Calcium, (b) phosphorus, and (c) strontium. (●) CP; (◊) CPS1; (▲) CPS5; (▽) CPS10.

the MAO process. It is generally known that oxide fusion results from the high temperature of the plasma-like state on the surface, and that the erupted gases oxygen and hydrogen can form a three-dimensional characteristic surface morphology of an oxide and a spongy interconnected microstructure [13]. As shown in Fig. 1, the MAO coatings containing strontium had a three-dimensional porous structure, which is beneficial for cell adhesion.

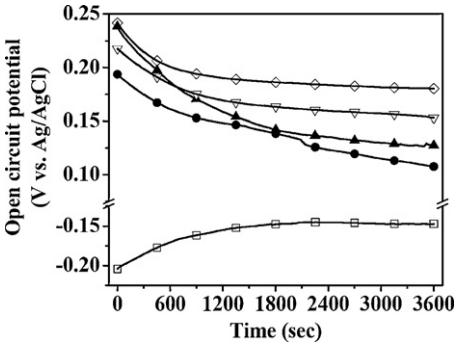

Fig. 7. Open circuit potential curves of specimens in SBF, 37 °C, pH = 7.4. (□) Ti; (●) CP; (◊) CPS1; (▲) CPS5; (▽) CPS10.

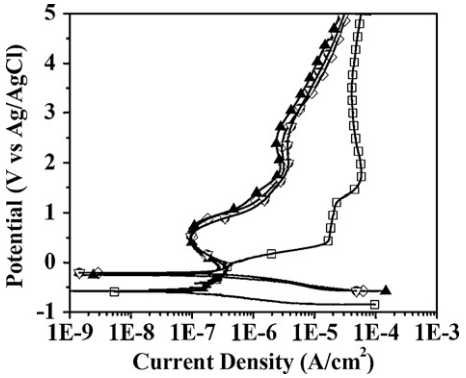

Fig. 8. Potentiodynamic polarization curves of specimens in SBF. (□) Ti; (●) CP; (◊) CPS1; (▲) CPS5; (▽) CPS10. At least 3 specimens were used for corrosion testing.

The surface composition of implants plays an important role on their biocompatibility and biological response of tissue. Clinical results of bone-implant interfaces show that bioactive implants form a bone-like apatite layer on their surface [14]. Previous studies showed that for apatite–wollastonite (A–W) glass ceramics soaked in SBF, the surface was covered with a layer of the apatite phase after 7 days of immersion [5–7]. When A–W glass ceramics were implanted into the tibias of rabbits, the interface between the A–W surface and bone was direct contact after 8 weeks [5]. The dissolution of Ca^{2+} and $HSiO_3^-$ ions from glass ceramics can form a Ca, P-rich layer to enable direct bonds with bone [6]. In the study of Song et al. [15], porous TiO_2 oxide films were fabricated on titanium via anodic oxidation with various acidic electrolytes. The bioactivity was examined by immersion in minimum essential medium solution. Immersion in SBF can mimic the reactions of samples exposed to a body environment, especially surface reactions. Many studies indicated that MAO coatings on the surface of titanium induce apatite formation upon exposure to SBF, exhibiting excellent bioactivity [16–18]. Therefore, the bioactivity of implant materials can be evaluated based on the formation of bone-like apatite on the surface.

As shown in Fig. 2, the apatite completely covers the surfaces of MAO coatings containing strontium. During the MAO process, the incorporation of phosphorus and calcium into the oxide coatings enhanced the formation of the apatite layer. However, the addition of strontium is possible to change the ability of apatite formation. A previous study demonstrated the dissolution behavior of hydroxyapatite containing 1–10 mol% strontium and found that solubility increased with increasing strontium content. The calcium ions released from MAO coatings containing strontium after immersion increase ionic activity and apatite precipitation. The incorporated phosphorus of MAO coatings might be hydrolyzed to the HPO_4^{2-} ionic species after immersion in SBF, attracting the cal-

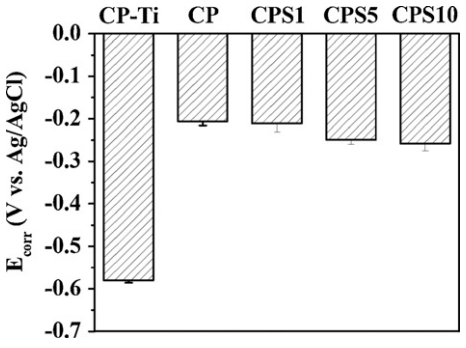

Fig. 9. Corrosion potential (E_{corr}) values of the specimens.

cium ion. The calcium ion release and phosphorus hydrolysis of two situations could occur simultaneously [19]. In the present study, the SEM results indicate that fiber-like structures start to deposit on the MAO coatings surface after 1 day of immersion, and that a continuous layer of precipitates fully covers the coatings surface after 7 days of immersion. The MAO coatings containing calcium, phosphorus, and strontium induce apatite formation on the surface within a short period of immersion in SBF. This indicates that the existence of strontium in the MAO coatings enhances the formation of an apatite layer on the specimen surface after immersion in SBF. The above result shows that the formation of the apatite on the MAO coatings surfaces will show the biocompatibility *in vivo*.

The XRD peak intensity of apatite for specimens of MAO coatings soaked in SBF for 1 day is shown in Fig. 3. Although the intensity of the apatite phase is not very apparent after 1 day of immersion, the intensity of the apatite phase increases with increasing immersion time. The apatite formation is not only a process of heterogeneous nucleation, but also depends on the supersaturation of the SBF solution. Besides, the morphology of MAO coatings surface also plays an important role in apatite nucleation. The concave sites of three-dimensional structures provide nucleation sites for bone-like apatite anchors [20]. This phenomenon explained that the three-dimensional structure combines compositions of coatings to accelerate apatite nucleation by increasing the ionic activity product of apatite. Therefore, the surfaces of MAO coatings were covered with apatite and the XRD peaks of apatite had similar intensities, as shown in Figs. 2 and 4. The inset in Fig. 2 shows that the apatite on the surfaces of MAO coatings had a fiber structure. A similar fiber structure was observed in previous studies [21,22]. Xue et al. [21] found that the Sr-HA surface appeared to be covered in apatite after being soaked in SBF for 3 days and that the fiber structure was the apatite phase. Apatite was observed on the surface of samples in a solution without strontium, exhibiting a fiber structure [22]. When the strontium content in the solution reached 1.0 mM, the morphology of the apatite changed. In the present study, after immersion for 7 days, the amount of strontium released from the CPS10 specimen was 0.065 ppm. This suggests that strontium in SBF solution does not inhibit the formation of apatite, as shown in Fig. 2. Due to the formation of apatite, the surface composition of calcium and phosphorus of the MAO coating increased after immersion in SBF, but the content of strontium decreased, as obtained from EDX analysis (Fig. 6). As shown in Fig. 5, the calcium and phosphorus concentrations decreased with increasing immersion time, whereas that of strontium increased. This result indicates that strontium was released from the coating into the solution.

Titanium implants stay in contact with body fluids and tissue for long periods of time, so their corrosion behavior must be determined. Implants made of titanium materials also release metal ions into the body. Messer et al. [23] exposed titanium implants to several solutions, and found that they had a risk of corrosion. Hence, coatings are necessary to protect the implants in a body environment. Using electrochemical methods, it could be predicted corrosion behavior of implants *in vivo*. As shown in Fig. 7, the continuous decrease of OCP for the four kinds of specimen in the initial stage indicates that the MAO coatings are not stable in the initial stage. The interface of the coating and solution undergoes a reaction, where the ions are released from the coating to supersaturation SBF solution. As shown in Fig. 2, the formation of apatite on the surface of MAO coating can be attributed to the dissolution behavior of coating. This indicates that the dissolution of calcium ions improves the formation of the apatite layer [7,19]. The polarization curves of the four kinds of MAO coating are similar, as shown in Fig. 8. This suggests that strontium in MAO coatings does not affect the corrosion properties. In the polarization curves, the four kinds of specimens exhibit a passive region. Furthermore, the MAO coatings exhibit a lower current density in the passive region. As shown in Fig. 9, MAO coatings have a significantly higher E_{corr} value than that of as-polished titanium. Baszkiewicz et al. [24] found that titanium surface modification by plasma electrolytic oxidation and hydrothermal treatment decreases the corrosion risk. The thick oxide layers of samples modified by MAO provided better corrosion resistance than that of non-modified titanium. The oxide layer of alkali-treated titanium improved corrosion resistance [25]. MAO coatings containing strontium showed the excellent corrosion resistance.

In this investigation, the coating containing strontium on the surface of titanium by micro-arc oxidation provide the great properties, including forming apatite ability and corrosion resistance. Because titanium and its alloy are widely in dental and orthopedic implant, these insights would be beneficial to the biomaterials designing by micro-arc oxidation technique.

5. Conclusions

The properties of MAO coating containing strontium on titanium substrate were characterized by TF-XRD, SEM/EDX, ICP-OES, and electrochemical measurement. The following experimental results were obtained:

(1) After the MAO process, open pores and three-dimension structures formed on the surface of the titanium substrate. EDX results indicate that calcium, phosphorus, and strontium became incorporated into the MAO coatings.
(2) After being soaked in SBF, the surface of MAO coatings was covered with precipitates, which were composed of fiber structures. TF-XRD analysis shows that the precipitate was the apatite phase. The intensity of the apatite phase increased with increasing immersion time.
(3) In the electrochemical test, the four kinds of MAO coatings showed similar polarization curves. Compared to as-polished titanium, the four kinds of MAO coatings have a more noble E_{corr} and lower current density in the passive region.

All measurements indicate the formation of apatite on the surface of MAO coatings, which is an essential characteristic of bioactivity. The MAO coatings release strontium into the surrounding environment, which is beneficial for bone formation.

Acknowledgments

The work has been financed by National Science Council, Taiwan, NSC 97-2221-E-006-005-MY2.

References

[1] T.M. Lee, J. Mater. Sci. Mater. Med. 17 (2006) 15–27.
[2] B. Kasemo, J. Laausmaa, Int. J. Oral Maxillofac. Implants 3 (1988) 247–259.
[3] L. Zhu, X. Ye, G.X. Tang, N.M. Zhao, Y.D. Gong, Y.L. Zhao, J.Z. Zhao, X.F. Zhang, J. Biomed. Mater. Res. 78A (2006) 515–522.
[4] C.S. Chang, T.M. Lee, C.H. Chang, J.K. Liu, Clin. Oral Implant Res. 20 (2009) 1178–1184.
[5] T. Kokubo, in: T. Yamamuro, L.L. Hench, J. Wilson (Eds.), CRC Handbook of Bioactive Ceramics, CRC Press, Boca Raton, FL, 1990, pp. 41–49.
[6] K. Ohura, T. Nakamura, T. Yamamuro, T. Kokubo, Y. Ebisawa, Y. Kotoura, M. Oka, J. Biomed. Mater. Res. 25 (1991) 357–365.
[7] T. Kokubo, Biomaterials 12 (1991) 155–163.
[8] L.L. Hench, J. Biomed. Mater. Res. 41 (1998) 511–518.
[9] M.C. García-Alonso, L. Saldaña, G. Vallés, J.L. González-Carrasco, J. González-Cabrero, M.E. Martínez, E. Gil-Garay, L. Munuera, Biomaterials 24 (2003) 19–26.
[10] Y.W. Li, J.C.Y. Leong, W.W. Lu, K.D.K. Luk, K.M.C. Cheung, K.Y. Chiu, J. Biomed. Mater. Res. 52 (2000) 164–170.
[11] C. Capuccini, P. Torricelli, F. Sima, E. Boanini, C. Ristoscu, B. Bracci, G. Socol, M. Fini, I.N. Mihailescu, A. Bigi, Acta Biomater. 4 (2008) 1885–1893.
[12] K.H. Nan, T. Wu, J.H. Chen, S. Jiang, Y. Huang, G.X. Pei, Mater. Sci. Eng. C 29 (2009) 1554–1558.
[13] J.P. Schreckenbach, G. Marx, F. Schlottig, M. Textor, N.D. Spencer, J. Mater. Sci. Mater. Med. 10 (1999) 453–457.

[14] P. Ducheyne, Q. Qiu, Biomaterials 20 (1999) 2287–2303.
[15] H.J. Song, S.H. Park, S.H. Jeong, Y.J. Park, J. Mater. Process. Technol. 209 (2009) 864–870.
[16] Z.W. Zhao, X.Y. Chen, A.L. Chen, M.L. Shen, S.M. Wen, J. Biomed. Mater. Res. 90A (2009) 438–445.
[17] J.F. Sun, Y. Han, K. Cui, Surf. Coat. Technol. 202 (2008) 4248–4256.
[18] W.H. Song, Y.K. Jun, Y. Han, S.H. Hong, Biomaterials 25 (2004) 3341–3349.
[19] J. Christoffersen, M.R. Christoffersen, N. Kolthoff, O. Bärenholdt, Bone 20 (1997) 47–54.
[20] J. Weng, Q. Liu, J.G.C. Wolke, D. Chang, K. DcGroot, J. Mater. Sci. Lett. 16 (1997) 335–337.
[21] W.C. Xue, J.L. Moore, H.L. Hosick, et al., J. Biomed. Mater. Res. 79A (2006) 804–814.
[22] A.L. Oliveira, R.L. Reis, P. Li, J. Biomed. Mater. Res. Part B: Appl. Biomater. 83B (2007) 258–265.
[23] R.L.W. Messer, G. Tackas, J. Mickalonis, Y. Brown, J.B. Lewis, J.C. Wataha, J. Biomed. Mater. Res. Part B: Appl. Biomater. 88B (2009) 474–481.
[24] J. Baszkiewicz, D. Krupa, J. Mizera, J.W. Sobczak, A. Biliński, Vacuum 78 (2005) 143–147.
[25] D. Krupa, J. Baszkiewicz, J. Mizera, T. Borowski, A. Barcz, J.W. Sobczak, A. Biliński, M. Lewandowska-Szumieł, M. Wojewódzka, J. Biomed. Mater. Res. 88A (2009) 589–598.